Crossovers in the Density of States of Fractal Silica Aerogels

R. Vacher,[1],[2] E. Courtens,[2] G. Coddens,[3] A. Heidemann,[4] Y. Tsujimi,[2],[a] J. Pelous,[1] and M. Foret[1]

[1]*Laboratoire de Science des Matériaux Vitreux, Université de Montpellier II, F-34095 Montpellier, France*
[2]*Zurich Research Laboratory, IBM Research Division, CH-8803 Rüschlikon, Switzerland*
[3]*Laboratoire Léon Brillouin, Centre d'Etudes Nucléaires de Saclay, F-91191 Gif-sur-Yvette, France*
[4]*Institut Laue-Langevin, 156 X, F-38042 Grenoble, France*
(Received 23 April 1990)

Combining neutron and Raman spectroscopies, we identify a succession of regimes in the vibrational dynamics of two aerogels of different microstructures. Aside from the phonon-fracton and fracton-particle mode crossovers, we find an additional crossover that suggests two distinct elastic regimes in the fracton range, which we associate with bending and stretching. Greatly different Debye-Waller factors are found in the two regimes, distinguishing them unambiguously in neutron spectra.

PACS numbers: 63.50.+x, 61.42.+h, 81.35.+k, 82.70.Gg

There is much current interest in comparing fracton predictions[1,2] to experiments on the vibrations of tenuous materials.[3] Real fractal solids consist of particles, of typical size a, distributed in a fractal manner up to a correlation length ξ, beyond which the materials are homogeneous. Thus, one recognizes three regimes for vibrations of characteristic length l, namely, phonons ($l > \xi_{ac}$), fractons ($\xi_{ac} > l > a$), and particle modes ($a > l$). Here, ξ_{ac} is the acoustical correlation length relevant to the vibrational problem, and which can be larger than the value ξ defined for the mass.[4] These regimes are separated by two crossovers. In addition, Feng has noted that the elasticity of tenuous materials should be dominated by stretching at small scales ($l < l_c$), and by bending at larger ones.[5] This should produce an additional crossover at l_c which was not yet observed in laboratory experiments. In this Letter, we present neutron and Raman vibrational spectroscopy results on silica aerogels. Correlating data over the entire frequency range of interest, and using gels of different microstructures, we identify for the first time a succession of regimes and crossovers.

Silica aerogels are excellent systems for the investigation of fractal vibrations, as explained, for example, in Ref. 6, in which earlier work is reviewed. Their structure, as revealed by small-angle neutron scattering (SANS), can exhibit an extended fractal range.[7] Brillouin scattering established anomalous dispersion near the phonon-fracton crossover at frequency ν_{col}.[8] Inelastic neutron scattering demonstrated the fracton-particle crossover at ν_{co2}, with an extended fracton regime.[9] More recently, neutron spin-echo (NSE) experiments confirmed the former crossover in the density of states (DOS).[10] Open questions remain as to the value of the fracton dimension $\bar{d}$, which characterizes the scaling with frequency of the fracton DOS, $\mathcal{N}(\omega) \propto \omega^{\bar{d}-1}$, where $\omega = 2\pi\nu$ is the angular frequency. Not only do $\bar{d}$ values appear to be nonuniversal, but different values of

$\bar{d}$ near ν_{col} and ν_{co2} were found in similar materials.[9,10] To clarify these points, we undertook an extensive study of the DOS on single well-characterized samples using neutron backscattering (BS) and time-of-flight (TOF) spectrometries. The experiments were performed on the instruments IN13 (BS) at the Institut Laue-Langevin in Grenoble, France, and Mibemol (TOF) at the Laboratoire Léon Brillouin in Saclay, France. Since numerical simulations suggest a strong dependence of $\bar{d}$ on the microstructure,[11] and as the latter can be modified appreciably by varying gel preparation,[12] we measured two distinct sample batches. One was obtained by hydrolysis of tetramethoxysilane without the addition of a catalyst ("neutral" reaction, labeled N), and the other was prepared with addition of ammonia to the reaction water (base catalyzed, B). Both batches were oxidized to remove remaining organic groups, and thoroughly dried as explained elsewhere.[9] Neutral preparation produces small particles and gels with rather tight microstructures, leading to fairly high fractal dimensions D. Base catalysis leads to larger particles and more tenuous microstructures.

Figure 1 displays the DOS obtained with sample N. The elastic structure factor $S(q)$, where q is the momentum transfer, is shown in the inset. Fits of $S(q)$ following Ref. 7 reveal an extended fractal region with $\xi \simeq 110$ Å and $D = 2.4 \pm 0.05$. From the onset of the Porod slope, $S(q) \propto q^{-4}$, the gyration radius of the particles is $R \simeq 6$ Å. This agrees with previous measurements[7] at the same density $\rho = 210$ kg/m^3. The low-frequency DOS curve results from a fit to the entire NSE data.[10] It shows ν_{col} and a fracton regime with an effective value of $\bar{d} = 1.4 \pm 0.1$. The high-frequency DOS is obtained from TOF spectroscopy at a neutron wavelength $\lambda = 8$ Å. The points shown have been measured at 160 K. Identical results within the error margin are obtained at 300 K. These data are derived from the purely incoherent contribution,[9] using the difference between signals mea-
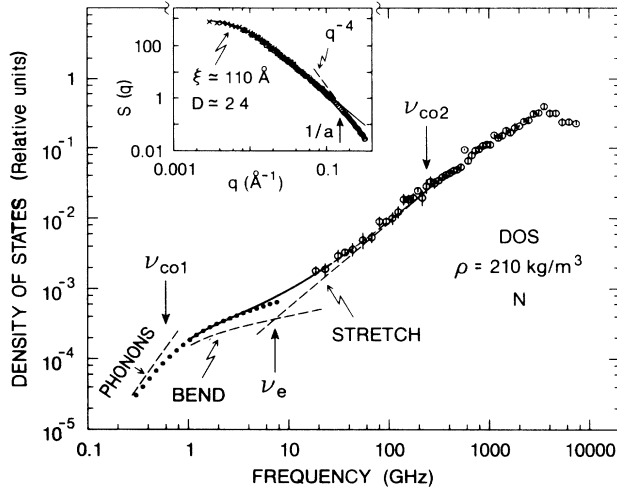
FIG. 1. The density of states $\mathcal{N}(\omega)$ of the neutrally prepared batch N. The open circles are TOF measurements. The dotted curve indicates the DOS that fits the NSE data. The solid line is a fit to the BS data presented here. This law is extrapolated as shown by the dashes throughout the high-frequency fracton region. The dashed lines indicate the asymptotic phonon as well as the independent bend and stretch contributions. Inset: SANS data from the same sample, fitted as described in Ref. 7. A straight line shows the Porod region at high q.
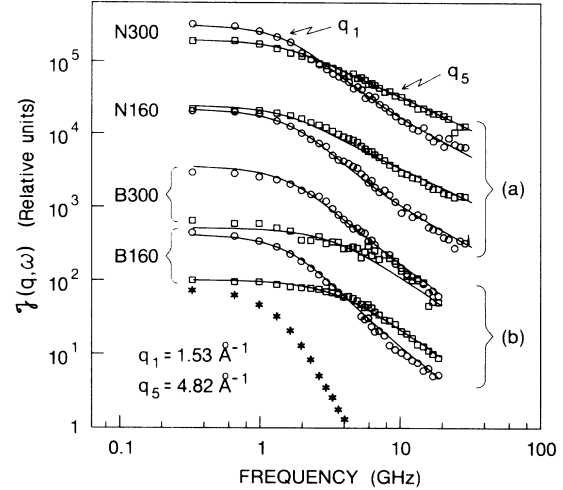

FIG. 2. Inelastic BS spectra at two wave vectors and two temperatures for samples (a) N, and (b) B. The lines are fits by Eq. (1) as discussed in the text. The successive pairs of curves have been shifted by factors of 10 to improve legibility. The lower curve (stars) is the IN13 instrumental function measured on vanadium.

sured on two samples from batch N, one with protons attached to the silica network (labeled NH), and the other with the protons substituted by deuterons (ND). The fracton range terminates at $\nu_{co2} \simeq 250$ GHz, as it is already known from Raman measurements.[13] Comparing NSE to TOF, one notes a clear change of slope in the DOS around 10 GHz. This is investigated next, using BS spectroscopy.

Typical inelastic BS spectra obtained on sample ND are shown in Fig. 2(a). Almost identical spectra are obtained with NH, which precludes gaining information from the difference ND $- N$H. This is related to the short incident neutron wavelength $\lambda \simeq 2.23$ Å of IN13. However, large q values are achieved at low ω transfer. The length scales corresponding to q are smaller than the particle size, whereas those associated with the excitations at ω are very much larger. Although the scattering at the scale of the particles is presumably coherent, the intensity related with long-wave excitations is in the harmonic limit well approximated by[14]

$$\mathcal{J}(q,\omega) \cong k_B T q^2 \sum_i A_i \exp[-\tfrac{1}{3} q^2 \langle u_i^2 \rangle] \mathcal{N}_i(\omega)/\omega^2 . \quad (1)$$

Since fractals are inhomogeneous in their very nature, the sum accounts for different local Debye-Waller factors, $\exp[-\tfrac{1}{3} q^2 \langle u_i^2 \rangle]$, with corresponding proportionality coefficient A_i, and DOS $\mathcal{N}_i$, while $k_B T$ is the thermal energy. If there were only one term, the q and ω dependences would factorize, which would produce parallel curves in the presentation of Fig. 2. Instead, a continu-

ous change of spectral shape with q is observed, as illustrated for the two extreme q values. The result at q_5 is compatible with a phonon-fracton crossover

$$\mathcal{N}(\omega) \propto \omega^2 [1 + (\omega/\omega_{col})^2]^{(\bar{\bar{d}}-3)/2} , \quad (2)$$

and a fairly large $\bar{\bar{d}}$. The form (2) is known to describe the crossover for both Brillouin[8] and NSE data.[10] However, the latter results as well as the q_1 curve of Fig. 2 indicate a significantly smaller value of $\bar{\bar{d}}$. All the data measured at five q and two T values can be fitted simultaneously to (1) and (2) convoluted with the resolution function, using only *two* terms in (1). Each is characterized by a square amplitude $\langle u_i^2 \rangle \propto T$, and distinct values of $\bar{\bar{d}}$ and ω_{col}. We associate the two contributions with the mechanisms dominating the fracton DOS at low and high frequencies (Fig. 1), and designate them by subscripts b and s, respectively. As discussed below, we relate them to bend- and stretch-dominated elasticities, with an "elastic" crossover at ν_e.

To fit the data, we selected $\bar{\bar{d}}_b = 1.3$ and $\bar{\bar{d}}_s = 2.2$, in accordance with the asymptotic behaviors shown in Fig. 1. We find that a single crossover, where $\nu_{col} \simeq 0.7 \pm 0.2$ GHz, and $\tfrac{1}{3} \langle u_b^2 \rangle = 0.33 \pm 0.3$ Å^2, $\tfrac{1}{3} \langle u_s^2 \rangle = 0.06 \pm 0.02$ Å^2 at room temperature, gives excellent fits. We note that ν_{col} is close to the Brillouin and NSE values of that sample,[8,10] although it is below the resolution of IN13. From the square of the amplitudes, it is clear that scattering at q_5 is dominated by the "s" process. The fit also gives the values of A_b and A_s, from which we calculate $\mathcal{N}(\omega) \propto \sum_i A_i \mathcal{N}_i(\omega)$ shown in Fig. 1. The NSE and TOF data have been translated along the vertical axis of Fig. 1 to match best the BS result. Also shown are the

asymptotic phonon behavior and individual b and s processes. The sum of the latter leads to an effective exponent for the NSE measurement which is slightly larger ($\cong 1.4$) than that extracted by scaling the crossover frequency, as has been done in Brillouin measurements ($\bar{\bar{d}}_b \cong 1.3$).[8] Conversely, it also leads to an effective exponent for the high-frequency fracton DOS which is slightly smaller than the asymptotic $\bar{\bar{d}}_s$ value. The intercept of the two processes determines $v_e \cong 10$ GHz. The smoothness of this crossover quantitatively explains the shape of the specific heat versus T up to several kelvin.[15]

Figure 2(b) shows BS results obtained on the deuterated sample BD of batch B. The DOS of the B material is shown in Fig. 3, where a SANS measurement is also displayed in the inset. It gives $\xi \cong 70$ Å, $R \cong 10$ Å, and $D = 2.2 \pm 0.1$. The density is $\rho = 95$ kg/m^3, which implies a narrow fractal region for a base-catalyzed aerogel.[16] This suffices, however, to produce a fracton regime fairly broad in ω, as illustrated by the Raman susceptibility $\mathcal{J}(\omega)/n(\omega)$, also shown in Fig. 3. Here, $\mathcal{J}(\omega)$ is the Raman intensity, and $n(\omega)$ is the Bose factor. These
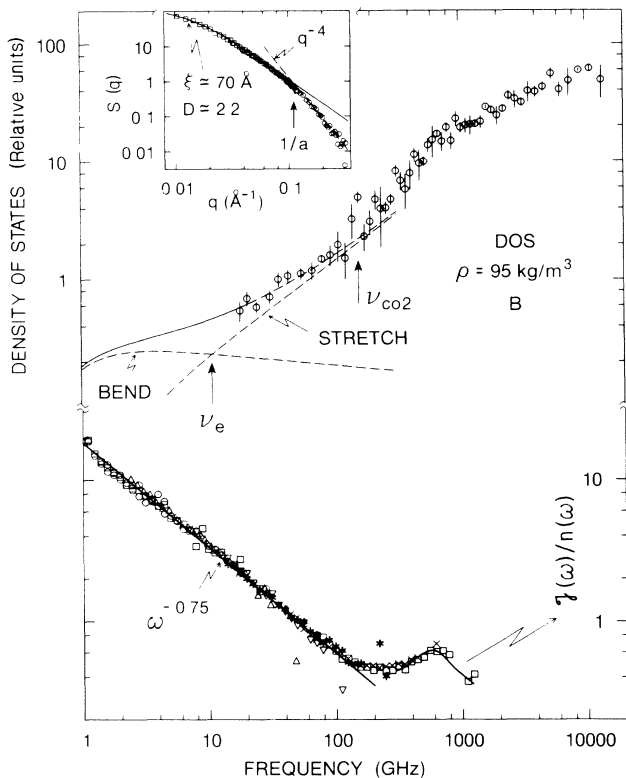
measurements are obtained in depolarized backscattering with an interferometer as done previously for N samples,[13] complemented above 300 GHz with a grating instrument. The main features of the Raman data are an extended fracton region with $\mathcal{J}(\omega)/n(\omega) \cong \omega^{-0.75}$, an onset of particle modes at about 100 GHz, and a broad particle peak around 600 GHz.

The high-frequency DOS of batch B was determined from the difference $BH - BD$. The fracton region of that measurement gives $\bar{\bar{d}}_s \cong 1.7 \pm 0.2$. Returning to Fig. 2(b), the presence of two components is again evident. Considering the curves at q_1, one notices that the slopes in the fracton region are much steeper than for the other batch. This implies a $\bar{\bar{d}}_b$ of ~ 1. A comparison of the curves at q_1 and q_5 suggests that there now could be two distinct values of v_{col}, one for b and one for s. The latter, at about 3 GHz, is well above the instrumental width, providing direct spectral evidence for the phonon-fracton crossover. The ten B spectra have been fitted with $\bar{\bar{d}}_b = 0.9$ and $\bar{\bar{d}}_s = 1.7$. The former value is suggested by simulations of tensorial elasticity on 3D percolation networks,[17] and the latter is from Fig. 3. The fits give $v_{col}^b \cong 0.8 \pm 0.2$ GHz, $v_{col}^s \cong 3 \pm 0.5$ GHz, and $\frac{1}{3}\langle u_b^2 \rangle = 0.82 \pm 0.04$ Å^2, $\frac{1}{3}\langle u_s^2 \rangle = 0.12 \pm 0.02$ Å^2 at room temperature. They allow calculation of the curve shown in Fig. 3. As in Fig. 1, the TOF data have been translated to match the BS result, and for the latter the independent contributions indicate a crossover v_e at about 10 GHz.

There is no sign of an anomaly at v_e on the Raman susceptibility. The same is true of the N batch.[13] The absence of feature at v_e in depolarized backscattering spectra is essential to the interpretation in terms of an elasticity crossover, as only bending modes substantially depolarize the light in that geometry. Hence, the susceptibility is dominated by modes of spectral dimension $\bar{\bar{d}}_b$, and its slope in the fracton regime is[13] $-2 + 2\sigma\bar{\bar{d}}_b/D$, where σ is an internal length dimension.[2] For both N and B, this gives $\sigma \cong 1.5$. An internal length dimension significantly larger than 1 suggests a very fractal microstructure.

Quite independently from the concept of a length-dependent elasticity crossover, as considered by Feng,[5] we have here introduced the idea of distinct spatial regions with different Debye-Waller factors. This is natural for a medium where vibrations are highly localized. Regions of high average frequency[6] have, by equipartition, low average vibrational amplitudes, and vice versa. This already applies independently of an elasticity crossover. However, our intuitive picture is that stretching dominates in highly connected regions, such as the backbone, and that bending is more important in less connected ones, such as floppy arms. Our results indicate then that bending-dominated regions have a much larger mean-squared amplitude $\frac{1}{3}\langle u^2 \rangle$ than stretching-dominated ones. Comparing the materials N and B, we

FIG. 3. Upper curve: The density of states $\mathcal{N}(\omega)$ of the base-catalyzed batch B. The open circles are from TOF measurements, and the solid line is a fit to the BS data, as in Fig. 1. Lower curve: Raman-scattering data. The various symbols refer to different spacings of the Fabry-Pérot interferometer (Ref. 13). The solid curve at the upper-frequency end is from a measurement with a grating spectrometer. The straight line is a guide to the eye. Inset: SANS data, as in Fig. 1.

also find that motions are larger for the more tenuous sample B. One could further speculate that the observed $v_{col}^b < v_{col}^s$ is related to an effectively shorter correlation length of the more tightly connected stretch-dominated regions. Naturally, this effect can be more important for more tenuous structures, with larger fluctuations in local environments.

In conclusion, we identified three crossovers and two distinct regions in the fracton regime of silica aerogels. The absence of additional crossover in Raman scattering suggests that the two distinct regions are caused by bend- and stretch-dominated elasticities, respectively. Further, the values of the spectral dimensions are clearly not universal. They are smaller for more tenuous samples. They also appear to be systematically smaller for bending as compared to stretching.

[a]Present address: Hokkaido University of Education, Hakodate, Hokkaido, Japan.

[1]S. Alexander and R. Orbach, J. Phys. (Paris), Lett. 43, L625 (1982).

[2]S. Alexander, Phys. Rev. B 40, 7953 (1989).

[3]See, e.g., T. Freltoft, J. Kjems, and D. Richter, Phys. Rev. Lett. 59, 1212 (1987); H. Conrad, U. Buchenau, R. Schätzler, G. Reichenauer, and J. Fricke, Phys. Rev. B 41, 2573 (1990); D. W. Schaefer, C. J. Brinker, D. Richter, B. Farago, and B. Frick, Phys. Rev. Lett. 64, 2316 (1990).

[4]E. Courtens and R. Vacher, Proc. Roy. Soc. London A 423, 55 (1989).

[5]S. Feng, Phys. Rev. B 32, 5793 (1985).

[6]E. Courtens, R. Vacher, and E. Stoll, Physica (Amsterdam) 38D, 41 (1989).

[7]R. Vacher, T. Woignier, J. Pelous, and E. Courtens, Phys. Rev. B 37, 6500 (1988).

[8]E. Courtens, R. Vacher, J. Pelous, and T. Woignier, Europhys. Lett. 6, 245 (1988).

[9]R. Vacher, E. Courtens, G. Coddens, J. Pelous, and T. Woignier, Phys. Rev. B 39, 7384 (1989).

[10]E. Courtens, C. Lartigue, F. Mezei, R. Vacher, G. Coddens, M. Foret, J. Pelous, and T. Woignier, Z. Phys. B 79, 1 (1990).

[11]J. Kieffer and C. A. Angell, J. Non-Cryst. Solids 106, 336 (1988).

[12]R. K. Iler, The Chemistry of Silica (Wiley, New York, 1979).

[13]Y. Tsujimi, E. Courtens, J. Pelous, and R. Vacher, Phys. Rev. Lett. 60, 2757 (1988).

[14]See, e.g., S. W. Lovesey, Theory of Neutron Scattering from Condensed Matter (Clarendon, Oxford, 1984).

[15]A. M. de Goër, R. Calemczuk, B. Salce, J. Bon, E. Bonjour, and R. Maynard, Phys. Rev. B 40, 8327 (1989).

[16]D. W. Schaefer and K. D. Keefer, Phys. Rev. Lett. 56, 2199 (1986).

[17]I. Webman and G. S. Grest, Phys. Rev. B 31, 1689 (1985).